SUPPLEMENTARY MATERIAL

1. Location of MODIS pixels used for each site

Table S1. Location of MODIS MCD43A4.006 pixel used for each study site.

Site	Eddy covariance tower location		MODIS pixel		
	Latitude	Longitude	Latitude	Longitude	Distance from tower (m)
Grassland	33.7365	-117.6946	33.7562	-117.7243	3514
Desert shrubland	33.6518	-116.3721	33.6562	-116.3710	498
Desert chaparral	33.6100	-116.4502	33.6104	-116.4491	At tower location
Coastal sage shrubland	33.7343	-117.6959	33.7354	-117.6907	497
Oak-pine woodland	37.1087	-119.7313	37.1104	-119.7348	At tower location
Pinyon-juniper woodland	33.6049	-116.4547	33.5937	-116.4466	1447
Oak-pine forest	33.8079	-116.7717	33.8062	-116.7701	At tower location
Ponderosa pine forest	37.0311	-119.2563	37.0312	-119.2550	At tower location
Sierran mixed conifer forest	37.0673	-119.1948	37.0687	-119.1990	At tower location
Subalpine forest	37.0671	-118.9871	37.0687	-118.9901	At tower location

2. Plant traits at the study sites

Table S2. Species sampled and their leaf traits.

Site	Sampling date 2019	Species	Leaves for site's LMA and W_c community weighted means			Leaves with photosynthesis measurements		
			n	LMA ± SD g cm^{-2}	W_c ± SD g cm^{-2}	n	A_{leaf} ± SD µmol m^{-2} s^{-1}	LMA ± SD g cm^{-2}
CSs	April 21 and 26	*Artemisia californica*	5*	0.0103 ± 0.0014	0.0155 ± 0.0011	5	12 ± 3.8	0.0112 ± 0.0005
CSs	April 21 and 26	*Eriogonum fasciculatum*	4*	0.0150 ± 0.0005	0.0203 ± 0.0012	5	21.2 ± 4	0.0157 ± 0.0019
CSs	April 21 and 26	*Leymus condensatus*	10	0.0086 ± 0.0020	0.0123 ± 0.0021	5	11 ± 6.1	0.0089 ± 0.0012
CSs	April 21 and 26	*Malosma laurina*	33	0.0097 ± 0.0019	0.0142 ± 0.0023	5	23.5 ± 9.8	0.0108 ± 0.0007
CSs	April 21 and 26	*Salvia mellifera*	32	0.0086 ± 0.0022	0.0159 ± 0.0027	5	20.4 ± 7.2	0.0099 ± 0.0014
Ds	May 1, 2, 11	*Cylindropuntia ramosissima*	7	0.1806 ± 0.0721	0.3776 ± 0.0987	0		
Ds	May 1, 2, 11	*Hymenoclea salsola*	10*	0.0111 ± 0.0019	0.0391 ± 0.0079	5	33.2 ± 9.2	0.0152 ± 0.0039
Ds	May 1, 2, 11	*Hyptis emoryi*	9	0.0103 ± 0.0018	0.0178 ± 0.0025	0		
Ds	May 1, 2, 11	*Justicia californica*	20	0.0092 ± 0.0034	0.0220 ± 0.0051	5	26.4 ± 6.9	0.0125 ± 0.001
Ds	May 1, 2, 11	*Larrea tridentata*	10*	0.0134 ± 0.0011	0.0207 ± 0.0014	5	10.3 ± 3.9	0.0169 ± 0.0021
Ds	May 1, 2, 11	*Parkinsonia florida*	10*	0.0074 ± 0.0005	0.0151 ± 0.0020	5	21.6 ± 2.8	0.011 ± 0.0012
Dc	May 9 and 10	*Erodium cicutarium*	5*	0.0050 ± 0.0007	0.0079 ± 0.0014	5	13.8 ± 5.6	0.0054 ± 0.0002
Dc	May 9 and 10	*Eriogonum fasciculatum*	10*	0.0119 ± 0.0020	0.0212 ± 0.0020	5	29.9 ± 3.5	0.023 ± 0.0029
Dc	May 9 and 10	*Purshia tridentata*	10*	0.0154 ± 0.0011	0.0248 ± 0.0013	5	18.2 ± 4.6	0.023 ± 0.0029
Dc	May 9 and 10	*Stipa speciosa*	5*	0.0092 ± 0.0006	0.0122 ± 0.0002	5	10.7 ± 2.1	0.0064 ± 0.0006
Dc	May 9 and 10	*Yucca schidigera*	25	0.1225 ± 0.0145	0.1585 ± 0.0164	0		
G	April 19, 24, 26	*Amsinkia menziesii*	10*	0.0059 ± 0.0006	0.0248 ± 0.0017	5	21.2 ± 6.5	0.0068 ± 0.0006
G	April 19, 24,	*Avena sp.*	24	0.0041 ± 0.0010	0.0142 ± 0.0037	5	22.4 ± 5	0.0042 ± 0.0006

	26							
G	April 19, 24, 26	*Brassica nigra*	21	0.0049 ± 0.0009	0.0190 ± 0.0040	5	30.2 ± 3.4	0.0053 ± 0.0007
G	April 19, 24, 26	*Bromus diandrus*	25	0.0039 ± 0.0006	0.0107 ± 0.0016	5	12 ± 3.6	0.0042 ± 0.0005
G	April 19, 24, 26	*Leymus condensatus*	0			2	26.3 ± 1.3	0.01 ± 0.0015
G	April 19, 24, 26	*Stipa pulchra*	6*	0.0097 ± 0.0031	0.0190 ± 0.0072	5	13.1 ± 4.1	0.0059 ± 0.0013
G	April 19, 24, 26	*Unidentified forb*	28	0.0048 ± 0.0007	0.0209 ± 0.0039	5	28.9 ± 3.2	0.0059 ± 0.0012
PJw	July 18 and 19	*Bernardia incana*	8*	0.0098 ± 0.0016	0.0134 ± 0.0016	4	5.7 ± 1.9	0.0106 ± 0.0011
PJw	July 18 and 19	*Juniperus californica*	3*	0.0719 ± 0.0079	0.0099 ± 0.0010	3	4.3 ± 0.2	0.0719 ± 0.0079
PJw	July 18 and 19	*Pinus monophylla*	36	0.0608 ± 0.0125	0.0632 ± 0.0095	5	1.2 ± 0.7	0.0679 ± 0.0186
PJw	July 18 and 19	*Quercus palmeri*	30	0.0180 ± 0.0041	0.0119 ± 0.0042	5	13.5 ± 3.9	0.0202 ± 0.0015
Sierra sites	TRY database	*Pinus contorta*					3.0	0.0227
Sierra sites	TRY database	*Pinus jeffreyi*					8.9	0.0240
Sierra sites	TRY database	*Pinus monticola*					8.2	0.0200
Sierra sites	TRY database	*Pinus ponderosa*					6.3	0.0234

Sites are CSs: coastal sage shrubland, Ds: desert shrubland, G: grassland, Dc: Desert chaparral, PJw: pinyon-juniper woodland. Measured traits are LMA: leaf mass per area, W_c: leaf water content, A_{leaf}: leaf photosynthesis. *Small-leaved species where LMA and W_c trait measurements were made on compound samples of several leaves. Each compound sample may contain tens to several tens of leaves/leaflets.

3. Details about the relationships between vegetation indices and gross primary production

The exploratory analysis of the data for each site indicate that linear regressions adequately describes relationship between Vegetation Indices (VIs) and Gross Primary Production (GPP) at the studied sites (see Figure S1-S3). For the relationship with NDVI, only two sites (grassland and coastal sage shrubland) showed some degree of curvature at the highest values of NDVI, although the linear regression explained 71-85% of GPP's variation (the highest r^2). The relationship for EVI and NIR_V was linear in all the sites.

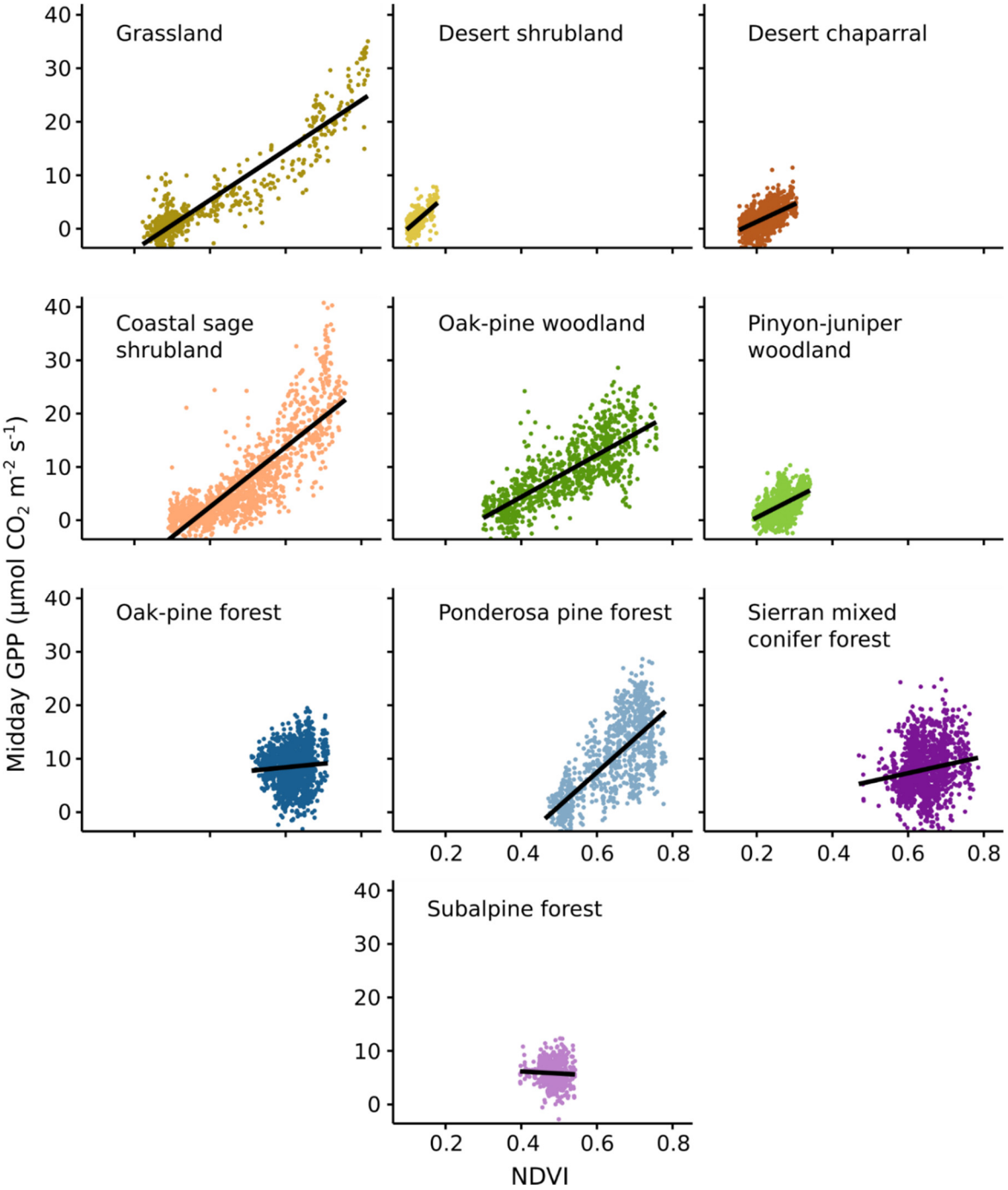

Figure S1. Relationship between NDVI and midday gross primary production for each site.

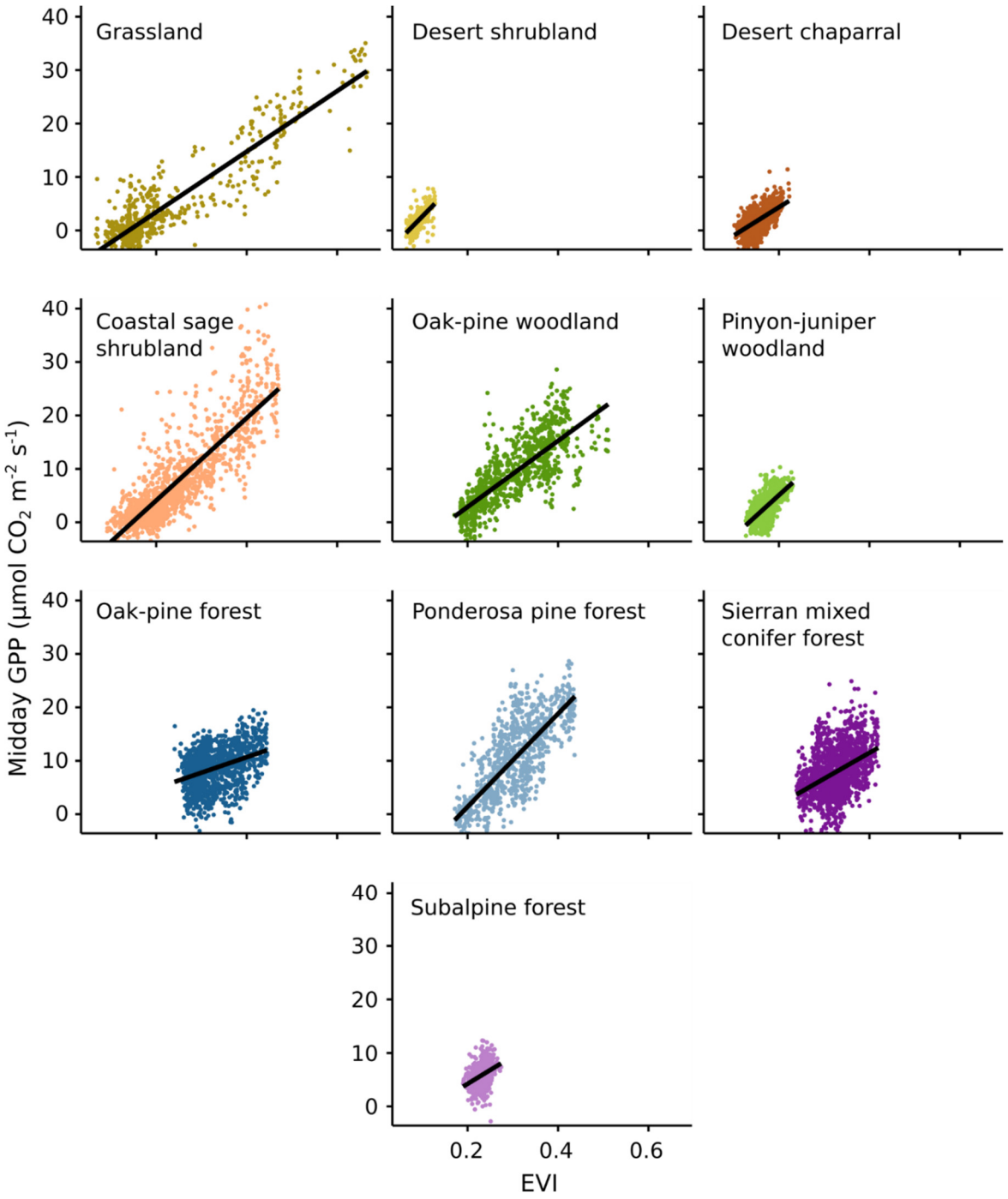

Figure S2. Relationship between EVI and midday gross primary production for each site.

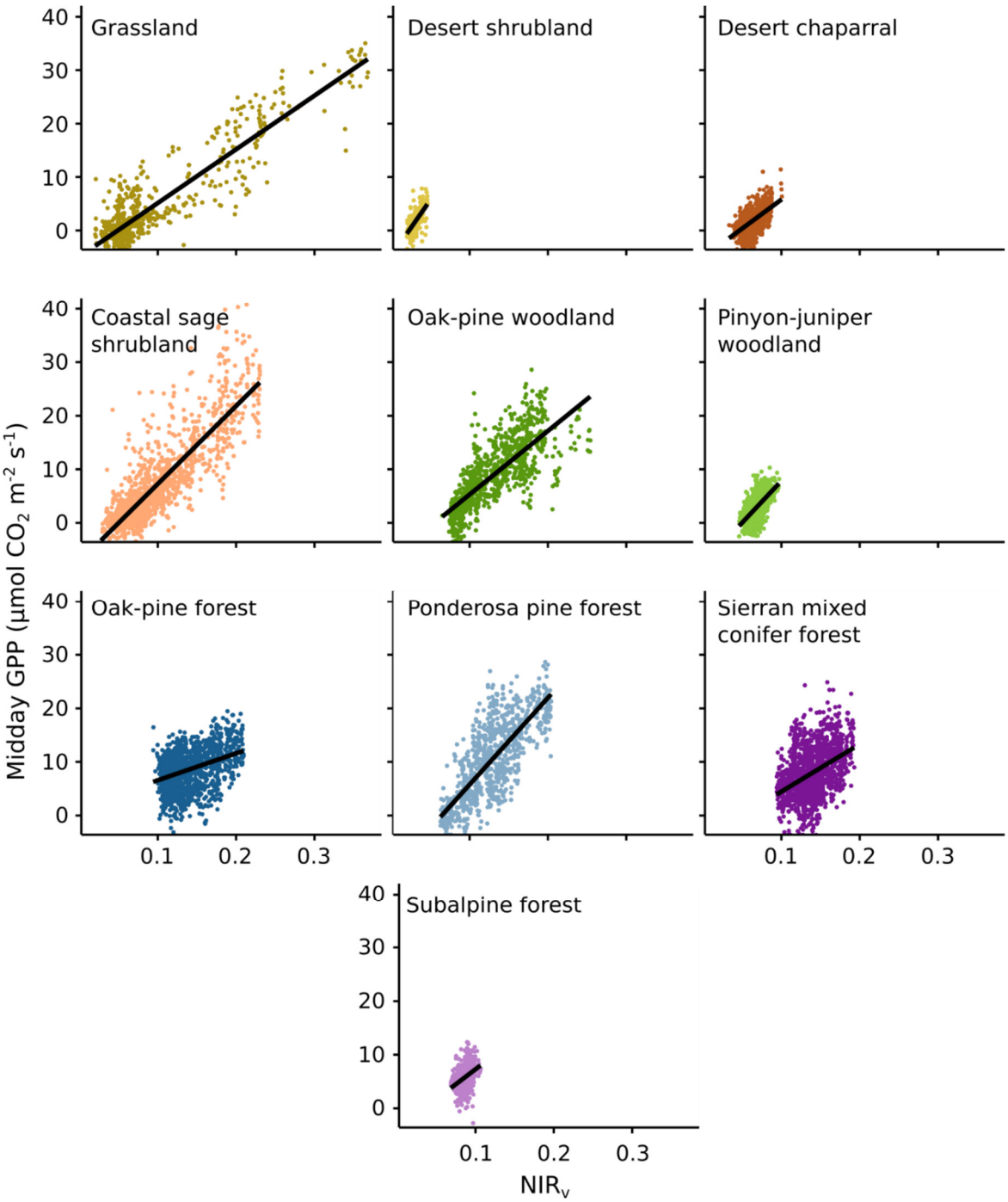

Figure S3. Relationship between EVI and midday gross primary production for each site.

Detailed information about the coefficients of the linear regressions between VIs and GPP for each site and across all sites is shown in Table S3. The observations in most of the sites do not homogeneously sample the their VI range, each site having more observations towards its lower end than towards the higher end (see Figures S1-S3). In addition, there are large differences in the number of observations available between sites, each sites having 5 to 12 years of observations. In order to minimize the impact of these issues on the results of our regression analyses, we performed our analysis as follows: for each site we 1) split the VI range of each site in 10 equally sized bins and took 10 random samples from each bin, 2) run the linear regression for each site with these more balanced samples and store the results, 3) then we run a linear regression for the samples taken for all the sites to estimate the across-sites relationships and store the results, 5) repeat all previous steps 200 times and average the obtained regression coefficients. Besides minimizing effects of unequal sampling within and across sites, this procedure allows using the entire dataset, and prevents that P values become meaningless with very large sample numbers. EVI and NIR_v have stronger within-site relationships in 9 of 10 sites, narrower ranges in its intercept and slopes, and stronger across-sites relationships.

We performed a similar procedure to provide an overall statistical measure that allowed us to compare the differences on within-site relationships across VIs. For this, we fitted the data to a statistical model evaluating the shared effect of the vegetation index across sites (equivalent to the across-site relationship), and the effect of site differences in the intercept (site effect) and slopes (interaction of site and VI): $= \beta_0 + \beta_1 \cdot VI + \beta_2 \cdot site + \beta_3 \cdot VI \cdot site + e$, where β are the statistical coefficients for each term. For a given VI, the percent of the overall GPP variance explained by site differences in intercepts and slopes (site + site-VI interaction effects) provides a measure of how different the relationships are between sites. This analysis was implemented on the same samples described above, and the results of the 200 runs were averaged. According to this analysis, site differences in intercepts and slopes in NDVI explain more than twice overall GPP variation (23.6 % variance explained) than in EVI (9.9 %) and NIR_v (8.4 %). These results, together with the narrower ranges in intercepts and slopes, support quantitatively that site/biome relationships for EVI and NIR_v are more convergent than for NDVI.

Table S3. Results of linear regression analyses for the temporal (single-site) and spatial (across-sites) relationships between vegetation indices and gross primary production.

Site	NDVI			EVI			NIR_v		
	r^2 (P value)	Intercept	Std slope*	r^2 (P value)	Intercept	Std slope*	r^2 (P value)	Intercept	Std slope*
Coastal sage shrubland	0.74 (<0.001)	-21.8	11.5	0.80 (<0.001)	-11.2	7.4	0.80 (<0.001)	-8.0	7.1
Desert chaparral	0.43 (<0.001)	-5.3	6.4	0.62 (<0.001)	-6.6	5.7	0.62 (<0.001)	-4.6	5.3
Desert shrubland	0.52 (<0.001)	-6.5	12.2	0.64 (<0.001)	-6.5	8.8	0.61 (<0.001)	-4.9	10.0
Grassland	0.83 (<0.001)	-16.1	9.6	0.87 (<0.001)	-7.5	5.4	0.88 (<0.001)	-4.7	4.8
Oak-pine forest	0.02 (0.401)	5.3	1.1	0.06 (0.066)	4.9	1.3	0.08 (0.022)	5.3	1.4
Oak-pine woodland	0.61 (<0.001)	-10.0	7.0	0.61 (<0.001)	-6.1	4.7	0.61 (<0.001)	-3.4	4.2
Pinyon-juniper woodland	0.39 (<0.001)	-7.0	7.1	0.67 (<0.001)	-9.4	7.0	0.72 (<0.001)	-8.9	8.1
Ponderosa pine forest	0.50 (<0.001)	-25.8	10.5	0.72 (<0.001)	-15.1	8.0	0.73 (<0.001)	-10.9	7.7
Sierran mixed conifer forest	0.08 (0.049)	-0.2	2.5	0.33 (<0.001)	-7.9	4.7	0.33 (<0.001)	-4.1	4.2
Subalpine forest	0.02 (0.455)	7.4	-0.6	0.29 (<0.001)	-4.0	4.1	0.25 (<0.001)	-1.6	4.2
Site minimum	0.02	-25.8	-0.6	0.06	-15.1	1.3	0.08	-10.9	1.4
Site maximum	0.83	7.4	12.2	0.87	4.9	8.8	0.88	5.3	10.0
Across-site relationship	0.47 (<0.001)	-3.5	4.3	0.68 (<0.001)	-5.3	4.7	0.71 (<0.001)	-3.3	4.6

* Slopes are not directly comparable when contrasting relationships from different vegetation indices because NDVI, EVI and NIRv have very different ranges of possible values. To make slopes comparable among relationships from different vegetation indices, we also regressed GPP against centered (on the mean across all sites) and scaled (to one standard deviation across all sites) vegetation indices data. We called the slopes obtained this way as "standardized slopes" (or Std. slopes). In particular, these standardized slopes allows an appropriate assessment of which vegetation index has more

consistent (similar) slopes among sites. The scaling and centering is not needed for a comparing intercepts because are always in the same units (the same units of gross primary production, μmol.

4. Analysis with Thornley (2002) and PROSAIL models

The GPP modeled with similar parametrization as in Figure 3b (see Appendix B) but including site-specific LAI and A_{leaf} closely follows the eddy covariance GPP measurements (Figure S4).

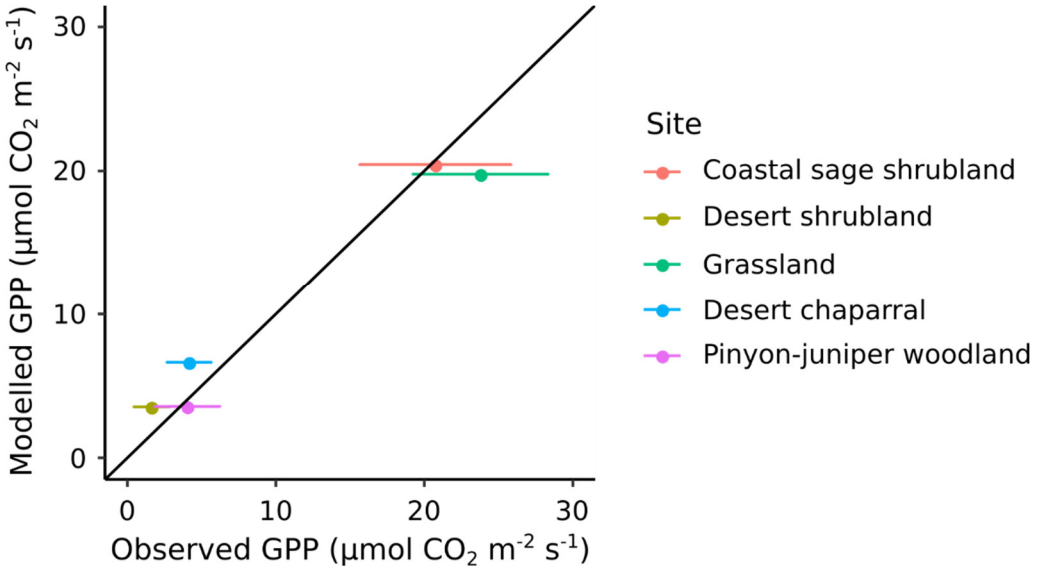

Figure S4. Comparison of observed and modelled midday gross primary production (GPP) at the study sites. Observed GPP is the mean ± 1 standard deviation of the cloudless eddy covariance observations taken under similar conditions (including similar vegetation indices). Modeled GPP is based on Thornley model and the *in-situ* observations of LAI and A_{leaf}.

The vegetation indices modeled from PROSAIL parametrized as in Figure 6 (see Appendix B), but with site-specific observations on soil reflectance (Figure S5), LAI and LMA, capture well the observed variation in vegetation indices at the study sites around the field sampling dates (Figure S6). The observed data for Figure S6 correspond to nine Landsat 8 pixels centered on the 90x90 sampling area at the study sites, obtained during clear conditions around the field sampling dates. The Landsat 8 surface reflectance data was obtained from the U.S. Landsat Analysis Ready Data (ARD) product CU_LC08, downloaded from https://lpdaacsvc.cr.usgs.gov/appeears/ and was filtered for cloud and aerosol conditions.

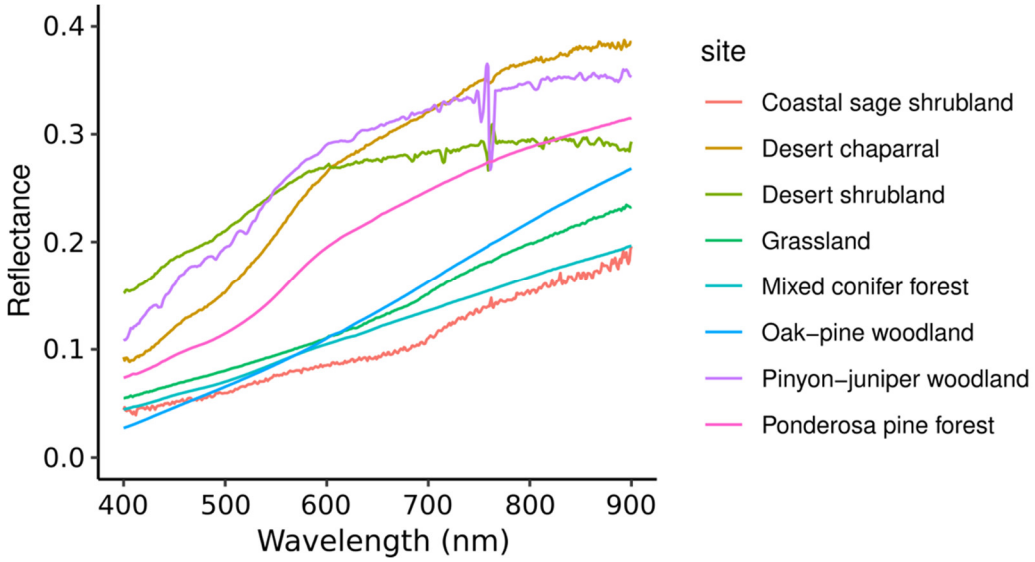

Figure S5. Soil reflectance spectra from the eddy covariance sites used in this study. We measured the soil reflectance at the five sites, and obtained supplemental observations from three of the other sites from Serbin et al ("NASA HyspIRI Airborne Campaign Leaf and Canopy Spectra and Leaf Traits", available at https://ecosis.org). Our study sites span a range of soil reflectance, with bright, sandy granitic soils at the desert shrubland, desert chaparral and pinyon-juniper woodland sites, and dark soils with higher organic content at the coastal sage shrubland, grassland, mixed conifer forest, and oak-pine woodland sites.

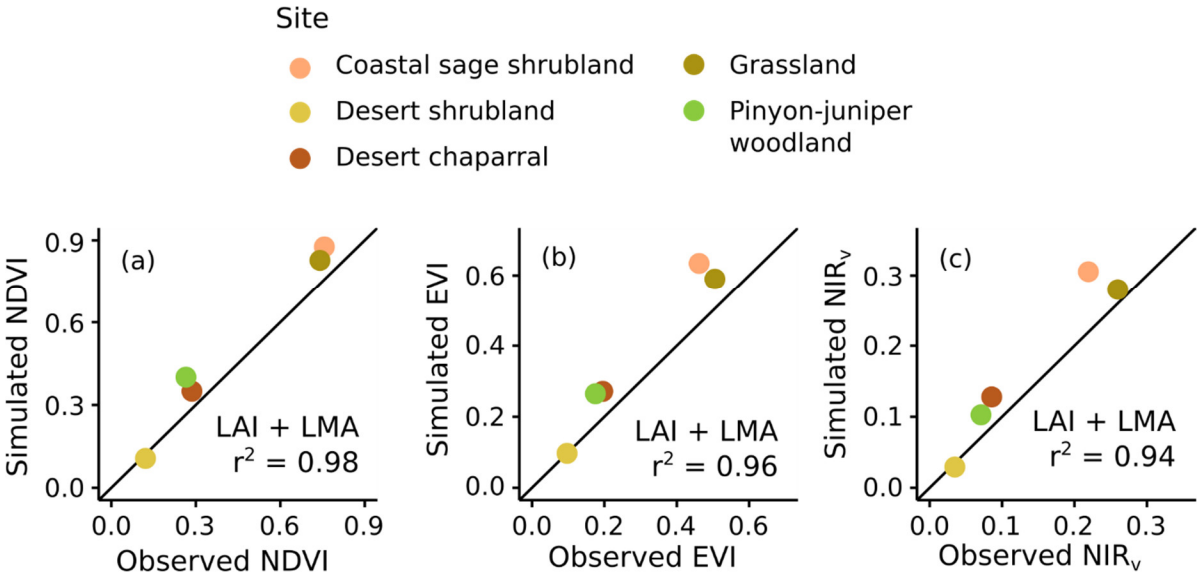

Figure S6. Comparison of observed vegetation indices from Landsat 8 with those modelled with PROSAIL parametrized with site-specific information of LAI, LMA and soil reflectance. Landsat 8 data were.

5. Leaf chlorophyll data from plant species from Southern California and Sierra Nevada

The leaf chlorophyll content per leaf area (C_{ab}) information used in analyses was based on existing datasets of leaf reflectance from five of our eddy covariance sites (dataset from Serbin et al). This data set contains measurements of shrub and tree species, including broadleaf and needleleaf, and either deciduous or evergreen, as well as grasses. We estimated C_{ab} from these measurements using the red edge chlorophyll index following Gitelson and Solovchenko (2017). The C_{ab} range found in this dataset (9-58 μg cm^{-2}, Figure S7) was used for the global sensitivity analysis.

Our analyses indicated that precise variation of C_{ab} across sites was not needed in our models to capture the observed variation in vegetation indices of the sites (see Figure 6b). For this reason, in some of the modeling analyses (Figure 6b-d) in our study we assumed a fixed C_{ab} value of 30 μg cm^{-2}, a value close to the mean from these data (Figure S7).

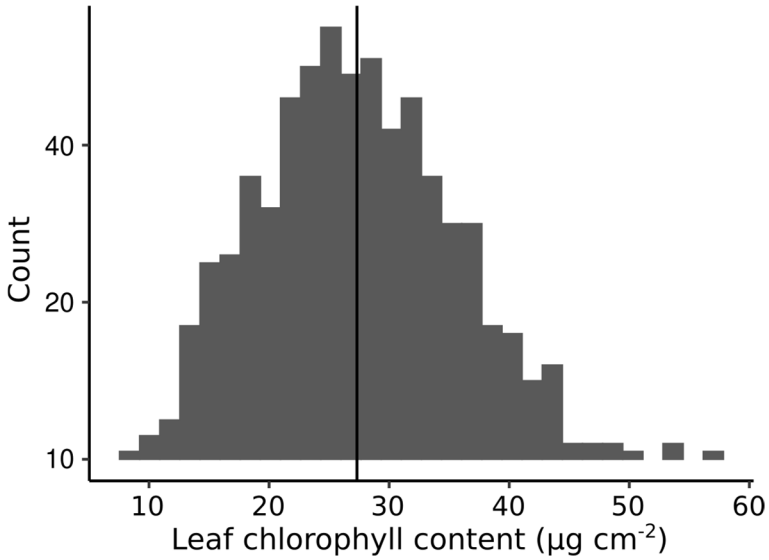

Figure S7. Histogram of leaf chlorophyll content per leaf area in species found in five of the eddy covariance sites. Solid line corresponds to the mean.

6. Correlations between vegetation indices: results from PROSAIL

We analyzed the correlations between vegetation indices from modeling results with PROSAIL. This allowed us to assess whether the correlations found between vegetation indices were specific to the conditions at our study sites, the specific satellite product used, or a more generalizable pattern supported by radiative transfer theory (Figure S8). We parametrized PROSAIL to model surface reflectance from all possible combinations from varying each parameter 5 steps over the same ranges used in the global sensitivity analysis (see Supplementary Material 1), and varying mean leaf angle over 10-80 º. This generated more than 78,000 simulations from the resulting combinations. The results show similar patterns to those obtained from the correlations in satellite data (Figure 7). This confirms that the strong similarity between EVI and NIR_V holds over a diverse combination of environmental and vegetation conditions.

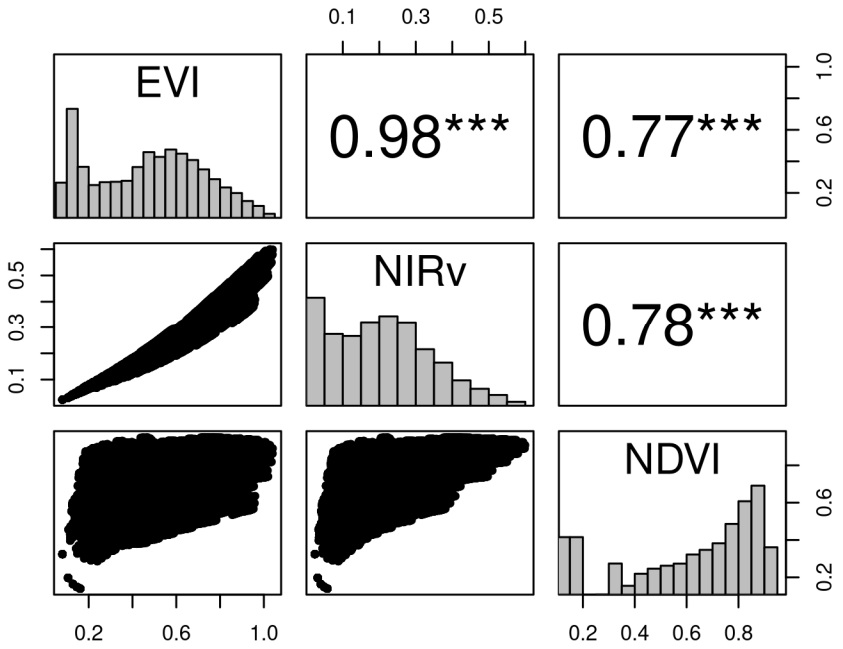

Figure S8. Correlation analysis between vegetation indices, using reflectance data modeled with PROSAIL.

7. Compilation of field measurements of mean canopy leaf angles

We compiled field measurements of mean canopy leaf angles from the literature to aid us in the selection of a range of values that well represent the variation found in this parameter across ecosystems. This dataset gathered 531 records from 48 publications, and included data from single-species and multi-species canopies from most major biomes (dataset available at Hinojo-Hinojo and Goulden, 2020). Only data from field-grown plants were included. When studies presented data on seasonal variation on mean canopy leaf angles from the same species/locations, the data were averaged and considered as a single record. The records were originally measured using several techniques, including clinometers and protractor measurements of individual leaves throughout the canopy, leveled photographs and digital measurement of individual leaves on image processing software, canopy hemispheric photographs, canopy analyzers (e.g. LAI-2000 and LAI-2200), and LIDAR. We excluded the data from BOREAS from our analysis (see Hinojo-Hinojo and Goulden, 2020). In our global sensitivity analyses, we used the range 10-90% percentile range of the dataset, which was 25-63º (Figure S9).

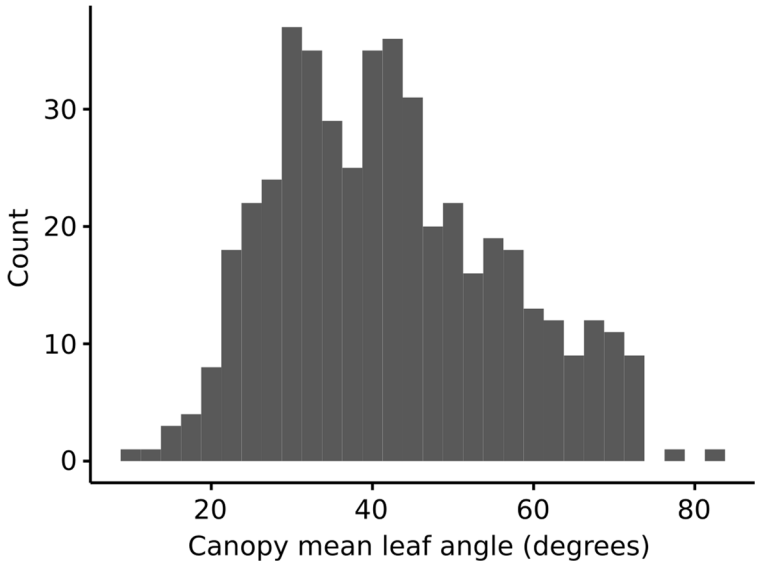

Figure S9. Histogram of the compiled dataset of mean canopy leaf angle

REFERENCES

Gitelson, A., Solovchenko, A., 2017. Generic Algorithms for Estimating Foliar Pigment Content. Geophys. Res. Lett. 44, 9293–9298.

Thornley, J.H.M., 2002. Instantaneous canopy photosynthesis: Analytical expressions for sun and shade leaves based on exponential light decay down the canopy and an acclimated non-rectangular hyperbola for leaf photosynthesis. Ann. Bot. 89, 451–458.

Hinojo-Hinojo, C, Goulden, M.L. 2020. A dataset of published measurements of canopy leaf inclination angles, UC Irvine, Dataset, https://doi.org/10.7280/D1T97H